

# Chapter 1

## Introduction

### 1.1 Interstellar extinction

#### 1.1.1 Physical origin & definition

As the light emitted from a star travels towards a distant observer, its intensity, or flux decreases with distance via an inverse-square law. Stars emit light across the full range of electromagnetic spectrum. Therefore, a beam of light from a star will consist of photons with an extremely wide range of wavelengths.

However, the interstellar medium (ISM) is not a perfect vacuum. It contains many different structures, such as clouds of diffuse gas and dust grains, that can absorb or scatter light passing through. For a given light source, this causes its brightness to appear lower than it would otherwise and changes the distribution of the same brightness with photon wavelength. The effect of dust clouds on optical light travelling towards observers is particularly apparent when examining star clusters and galaxies (including the Milky Way), with the dust obscuring optical light from sources behind the clouds.

Interstellar extinction is defined physically as the magnitude of the flux absorbed or scattered by the intervening line-of-sight ISM. Mathematically, extinction,  $A$ , is defined using the standard astronomical system of flux magnitudes via the following equation:

$$m - M = 5 \log \left( \frac{d}{\text{pc}} \right) - 5 + A \quad (1.1)$$

where  $m$  is the apparent magnitude of the source,  $M$  is its absolute magnitude and  $d$  is the distance to the source.

When a broadband beam of light passes through a cloud, the loss of flux due to absorption, refraction or diffraction is related to the optical depth,  $\tau$ . The optical depth is defined along the line-of-sight via:

$$\tau(l) = \int_0^l \rho \kappa dl = \int_0^l n \sigma dl \quad (1.2)$$

where  $l$  is the length of the path taken by the beam through the cloud,  $\rho$  is the mass density of the local cloud material,  $\kappa$  is the material's opacity,  $n$  is the particle number density and  $\sigma$  is the particle collision cross-section.

It should be noted that all quantities in the integrands in Equation 1.2 depend on local conditions at each point in the path travelled by the beam. In particular, the opacity, for a given wavelength, depends strongly on the available configurations for the atomic electrons in the cloud, which in turn depend on the chemical composition of the cloud. Although the light absorbed by atomic electrons is re-radiated, for a large number of electrons this radiation is emitted isotropically, causing a net decrease in the flux travelling in the direction of a given observer.

The quantities in Equation 1.2 therefore cannot be immediately discounted as being constant along the entire path required for the integration, let alone throughout the entire cloud. Furthermore, the dependence of opacity, and subsequently optical depth, on the composition of the medium causes a variation of its value with the wavelength of photons in the beam. This necessitates the specification of the optical depth being applicable for  $X$  in Equation 1.2.

The variation in flux of the light beam with distance travelled through the cloud is best expressed using the optical depth:

$$f = f_0 e^{-\tau} \quad (1.3)$$

where  $f$  is the flux of the beam after it exits the cloud and  $f_0$  is the flux at the point where the beam first encounters the cloud (i.e., at  $l = 0$ ). Returning to the equation for flux magnitudes given in Equation ??, we can use the relation in Equation 1.5 to rewrite Equation ?? as:

$$A = m - m_0 = -2.5 \log \left( \frac{f}{f_0} \right) = -2.5 \log(e^{-\tau}) \quad (1.4)$$

Therefore, we can define the extinction in terms of the distance travelled through, and the composition of, the ISM, both of which are accounted for in the optical depth:

$$A = 2.5 \log(e) \times \tau = 1.086 \tau \approx \tau \quad (1.5)$$

In conclusion, to a first-order approximation, the extinction is equal to the optical depth along the line of sight. Hence, the mathematical representation of extinction is proven to be aligned with its physical definition as the flux of photons scattered and absorbed in the interstellar medium.

The incidence of absorption and scattering events depends on the wavelength of the incoming photons. This dependence is also incorporated into the optical depth via the scattering cross-section  $\sigma$  in Equation 1.2. If the particles in the ISM are assumed to be spherical with radius  $a$ , its geometric cross-section is  $\pi a^2$  for any incoming photon. Using the scattering and geometric cross-sections, a dimensionless extinction coefficient:

$$Q(\lambda) = \frac{\sigma(\lambda)}{\pi a^2} \quad (1.6)$$

can be defined. When the photon wavelength is on the order of the particle size ( $\lambda \sim a$ ), Mie (1908) showed that  $Q \sim a/\lambda$ . In the limit  $\lambda \gg a$ ,  $Q$  decreases to zero, while for  $\lambda \ll a$ ,  $Q$  becomes constant with regard to wavelength. This shows that, for extinction in the UV-to-near-IR spectral range, which covers approximately a 100-1000 nm wavelength range, the scattering cross-section for relevant ISM atomic species is proportional to  $1/\lambda$  and is therefore significantly greater in the UV than in the IR. Therefore, referring back to Equation 1.5, interstellar extinction is also greater at shorter wavelengths, causing the source star to appear redder than its true colour (see Section 1.3). Hence, the effect of extinction is sometimes referred to as “reddening”.

A beam containing photons with a sufficiently large range of wavelengths will therefore lose some of its photons, and therefore flux, due to interactions with the ISM through which it travels. The magnitude of loss is determined by the wavelength(s) of those photons, the fraction of the beam consisting of these photons and the state of the ISM. For a given source, its interstellar extinction value represents the total flux absorbed or scattered due to all extinction events along the line-of-sight between the source and the observer.

### 1.1.2 Empirical extinction curves

The variation of extinction with wavelength discussed in the previous section has been studied for decades. Various authors have produced empirical results intended to better model the changes in the magnitude of extinction over an extended wavelength range, as explicit functions of wavelength or as values or functions unique to each in a selection of photometric filters.

Rieke & Lebofsky (1985) found that outside dense molecular clouds, which have high opacities and whose lines-of-sight are less frequently used as a result, all extinction laws for all Johnson filters studied were uniform between wavelengths of 1 and 13  $\mu\text{m}$  when observing sources in the direction of the Galactic Centre. This result was then used to produce constant  $A_X/A_V$  extinction ratios in the same filters. They also determined the now-widely used global average value of 3.08 (3.1) for  $R_V = A_V/E(B-V)$ , known as the total-to-selective extinction ratio, for the diffuse ISM.

Cardelli et al. (1989) used observations of mostly O- and B-type main-sequence stars to produce empirical equations describing the mean ratio of extinction coefficients at a specific wavelength  $\lambda$  ( $A_\lambda$ ) to the extinction in the Johnson- $V$  filter ( $A_V$ ), respectively. From this point onward, this ratio will be referred to as  $A_\lambda/A_V$ . They produced a basic equation of the form:

$$A_\lambda/A_V = a(x) + b(x)/R_V, \quad (1.7)$$

where  $x \equiv 1/\lambda$  and  $R_V \equiv A(V)/E(B-V)$ . The significance of  $R_V$ , as noted in the same paper, comes from its usefulness as an indicator of the nature of the interstellar medium through which the observed light travels in order to reach the observer. The total wavelength range was divided into 4 sub-ranges, each with a governing pair of empirically-determined equations to calculate  $a(x)$  and  $b(x)$ , respectively. The resulting extinction-ratio profiles for three lines of sight are displayed in Figure 1.1. This model underpins more recent studies of intrinsic effects on extinction (Girardi et al., 2008; Casagrande & Vandenberg, 2018), and provides the basis for the synthetic  $A_X/A_V$  datasets in this project. Equation 1.7 has become a standard model for theoretical studies to employ for predictions made in the UV, optical and near-IR wavelength regions, although it is not always accurate (O'Donnell, 1994; Fitzpatrick, 1999).

O'Donnell (1994) found deviations from the Rieke & Lebofsky (1985) extinction law in the soft-UV spectral range using a sub-sample of 22 stars from the same dataset. This was attributed to the uncertainty in the short-wavelength cutoff of the UV-range Johnson  $U$  filter and to the presence of the Balmer discontinuity within the limits of the filter bandpass.

Fitzpatrick (1999) found that, due to the broadband nature of the Johnson filters and the general decrease of extinction with wavelength, the Cardelli et al. (1989) relations overestimate the extinction in the near-IR and blue-visible Johnson filters. The study put forward corrections to the equations for  $a(x)$  and  $b(x)$  for these wavelength regions. However, in the UV region covered by the Cardelli et al. (1989) equations, the equations are accurate for 93% of a homogeneous UV observational database (Valencic et al., 2004).

Girardi et al. (2008) produced data tables of  $A_X/A_V$  for stellar atmosphere models with parameters  $T_{\text{eff}}$ ,  $\log(g)$  and  $[\text{Fe}/\text{H}]$ . They carried this out using the same ATLAS9 data (Castelli & Kurucz, 2004) that was used to generate the data for this project, but also combined it with data from other studies Girardi et al. (2002), resulting in data covering a parameter space extending beyond the ATLAS9 limits in all three parameters. They used the data tables to calculate the  $A_X/A_V$  values for the stellar models in Padova theoretical isochrones. While determining that the values of  $A_X/A_V$  varied significantly with  $T_{\text{eff}}$  and  $\log(g)$ , the variation with metallicity was found to be 0.17% between  $[\text{Fe}/\text{H}] = 0.0$  and  $[\text{Fe}/\text{H}] = -2.5$ . They found that, when they set  $A_V = 6$ , there was a systematic shift for the ACS system between extinction values calculated star-

wise using the tables of  $A_X/A_V$  data and a constant extinction value. The constant values of  $A_X/A_V$  were calculated from a yellow dwarf in the low-extinction regime. Overall, the  $A_X/A_V$  tables produced a smaller extinction coefficient in the F814W filter and a larger (F475W-F814W) colour index value. It also caused a change in the shape of the curve at the MSTO. They then applied the data from the tables to the case of the globular cluster M92. They found the optimal metallicity to be  $Z = 0.0004$  ( $[\text{Fe}/\text{H}] \approx -1.6$ ) instead of the value obtain by previous observers of  $Z = 0.0001$  ( $[\text{Fe}/\text{H}] \approx -2.2$ ). Therefore, their use of  $A_X/A_V$  data caused the estimated cluster metallicity to be greater than when using the standard one-size-fits-all approach to extinction.

Casagrande & Vandenberg (2014, 2018a, 2018b) created simple models for the parameter  $R_X = \frac{A_X}{E(B-V)}$ , consisting of a quadratic variation with effective temperature and a linear variation with metallicity (they found no significant variations with surface gravity) in multiple telescope filter systems. This was based on MARCS model stellar atmospheres, which have an upper  $T_{\text{eff}}$  limit of 8000K (Gustafsson et al., 2008). The equation is independent of surface gravity and has the following form:

$$R_X = a_0 + T_4(a_1 + a_2 T_4) + a_3 [\text{Fe}/\text{H}] \quad (1.8)$$

where  $T_4 = 10^{-4} \times T_{\text{eff}}$ . The equation is valid for  $5250\text{K} \leq T_{\text{eff}} \leq 7000\text{K}$ . Although these models are mathematically simple (with only 4 coefficients), the limited  $T_{\text{eff}}$  range in which they are applicable is problematic, particularly in the red giant branch (RGB) and lower main sequence of any stellar population.

## 1.2 Extinction in stars & stellar populations

### 1.2.1 Stellar parameters affecting extinction

This project examines the effect of extinction treatment methods on interpretations of observed stellar populations. To understand the effect of different stellar types with respect to the calculated interstellar extinction, we must first define the fundamental parameters that describe a stellar atmosphere, which will be used in this project as the input variables on which any star-to-star variations in extinction will be modelled.

The effective temperature ( $T_{\text{eff}}$ ) of a star is defined as the thermodynamic temperature of a black body which produces the same stellar flux across all wavelengths (known as the bolometric flux) as that produced by the star. The equation of the radiation emitted by a black body produces the body's flux per unit wavelength per unit angular viewing area,  $F_{\lambda,bb}$ , known as the black body's monochromatic flux. The equation, known as the Planck Law, is as follows:

$$F_{\lambda,bb} = \frac{2hc^2}{\lambda^5 \left( \exp \left( \frac{hc}{\lambda k_B T} \right) - 1 \right)} \quad (1.9)$$

where  $T$  is the thermodynamic temperature of the black body,  $h$  is Planck's constant,  $c$  is the vacuum speed of light and  $k_B$  is Boltzmann's constant. This equation also holds if the light wave frequency is used instead of the wavelength, with the monochromatic flux  $F_{\nu,bb}$  now being the black body flux per unit frequency:

$$F_{\nu,bb} = \frac{2h\nu^3}{c^2 \left( \exp \left( \frac{h\nu}{k_B T} \right) - 1 \right)} \quad (1.10)$$

In this project, the definition of monochromatic flux for any given object will be reserved exclusively for the flux per unit wavelength,  $F_{\lambda}$ , with any calculations involving black body fluxes using Equation 1.9.

The general approximation of stars to black bodies (and hence the actual stellar surface temperature to  $T_{\text{eff}}$ ) is valid because all stars have been observed to have spectra that closely resemble those of black bodies, with the notable exception of atmospheric absorption lines. The (intrinsic) luminosity of a star is used to define the effective temperature via:

$$L = 4\pi R^2 \sigma_{SB} T_{\text{eff}}^4 \quad (1.11)$$

where  $R$  is the (mean) stellar radius. Effective temperature has an effect on interstellar extinction due to its strong effect on the stellar luminosity and, hence, the flux, via the Planck Law in Equation 1.9. For a higher effective temperature, there will be more photons in the broad beam of light with wavelengths that make them likely to interact with the local ISM.

Different chemical elements have different orbital configurations of atomic/ionic electron states. Each electron state absorbs and emits photons at a particular wavelength, which varies between individual states and between elements. Therefore, a greater proportion of light in a broadband beam is absorbed in a medium containing a mixture of many different elements than in a medium dominated by one or two elements. From astrophysical observations, it is clear that hydrogen is by far the most abundant element in the universe, with helium a clear-but-distant second. The metallicity of a star is defined as the fractional abundance of heavy elements, often approximated by iron (Fe) alone, relative to the star's hydrogen (H) abundance, compared to that of the Sun. The abundances are determined by the strength of the elements' characteristic atomic absorption lines in the stellar spectra.

$$[\text{Fe}/\text{H}] = \log \left( \frac{N_{\text{Fe}}}{N_{\text{H}}} \right) - \log \left( \frac{N_{\text{Fe},\odot}}{N_{\text{H},\odot}} \right) \quad (1.12)$$

For a generic atomic species  $E$ ,  $N_E$  represents its number density. For stellar observations,  $N_E$  is measured at the surface. Since the output is logarithmic, a value of  $[\text{Fe}/\text{H}] = 0$  indicates solar metallicity. An increase in metallicity would cause the corresponding absorption lines to be stronger, thus reducing the observable flux. An increased metallicity also implies an increase in abundance of sub-ferrous metals. The presence of more nuclear species, each with unique absorption line configurations, inevitably creates more observable lines, further increasing the apparent extinction in the spectral flux. The effect of this reduction in flux manifests itself as a reduction in the stellar luminosity and therefore the effective temperature when all other stellar properties (such as the mass and age) are fixed. The position of the star

The definition of the stellar surface gravity  $g$  is simply the value of the standard Newtonian gravitational acceleration, applied to the stellar surface (the mass is the total stellar mass,  $M_*$ , and the distance is the stellar radius,  $R_*$ ):

$$g = \frac{GM_*}{R_*^2} \quad (1.13)$$

A greater surface gravity, as can be inferred from Equation 1.13, represents a surface with a higher mass density. For stars, being self-gravitating, this infers a higher atomic number density.

The effects of surface gravity on the stellar emission spectrum arise directly from the quantum properties of the interactions between the photons and atomic electrons in the stellar atmosphere.

When a particle, such as an electron, absorbs a photon, the absorption process is not instantaneous and therefore carries an uncertainty in the time taken for the process to be completed, with a corresponding uncertainty in energy due to the Heisenberg uncertainty principle. Across a large number of absorptions for the same initial electron state, the result is a spread in the energies of the absorbed photons. The associated emission line is therefore broadened by the multiple wavelengths of the photons. This is universal and referred to as “natural broadening”.

The impact of surface gravity arises via additional broadening effects upon these same absorption lines. When broadening effects are applied to an emission spectrum, such as a spectrum from a stellar surface, the result is that fewer photons pass through the surface, thereby reducing the surface flux seen by an outside observer.

The impact of stellar effective temperature, metallicity and surface gravity on extinction arises through their described effect on the spectral energy distribution (SED) emitted by the stellar atmosphere. Since both the SED and the magnitude of the interstellar extinction are functions of wavelength, different stellar types, with different SEDs, can be impacted to different extents by interstellar extinction at a given

wavelength.

### 1.2.2 Forbes effect

The Forbes effect occurs as a broadband beam of light, such as that passes through an extended partially-transparent medium, such as the Earth's atmosphere or an interstellar gas or dust cloud. It states that the greater the distance travelled by a light beam through the medium, the more penetrating the beam becomes (Forbes, 1842). The physical basis for this effect is that those photons in the original beam with wavelengths that make them the most likely to be absorbed or refracted are separated from the beam earlier. Therefore, as the beam travels through the medium, its constituent photons are progressively less likely to be interact with the medium (Grebel & Roberts, 1995). Since a higher fraction of its photons are retained as the distance through the medium increases, the beam is more penetrating (Ohvri et al., 1999).

This has the effect of producing a non-linear increase in extinction for one filter relative to the increase in another (Grebel & Roberts, 1995; Girardi et al., 2008). It should be emphasised that the Forbes effect occurs regardless of the source star's spectral type, and therefore represents an additional source of uncertainty when calculating extinction for highly-reddened stellar populations.

### 1.2.3 Determining properties of stellar populations

#### The role of CMDs

If we compare the individual black body spectra in Figure 1.2, it can be seen that the maximum monochromatic flux of the black body occurs at an increasingly shorter wavelength for objects with increasingly higher temperatures. This makes the object appear bluer to an observer. The relationship between the wavelength at which the monochromatic flux is maximal ( $\lambda_{max}$ ) and the black body temperature is quantified by Wien's displacement law:

$$\lambda_{max}T = 2.898 \times 10^6 \text{ nm K} \quad (1.14)$$

More importantly, Figure 1.2 demonstrates that, within the UV-to-IR wavelength regime, the change in monochromatic flux between values at two different wavelengths is always greater for stars with higher effective temperatures. Therefore, to measure a star's effective temperature, observers compare the star's observed flux in two filters operating at different wavelengths within this range. The difference between the star's flux magnitudes in each of the two filters is then taken, with the flux in the redder filter being deducted from that of the bluer filter. This quantity is known as the colour index. For two filters  $X$  and  $Y$ , with  $X$  being bluer than  $Y$ , the colour index of observations made using those filters,  $(X - Y)$ , is defined as:



$$\begin{aligned}
(X - Y) &= m_X - m_Y \\
&= (m_{X,0} - m_{Y,0}) + (A_X - A_Y) \\
&= (X - Y)_0 + E(X - Y)
\end{aligned} \tag{1.15}$$

where  $(X - Y)_0$  is the true or intrinsic colour index of the object and  $E(X - Y) = A_X - A_Y$  is known as the colour excess, but can also be denoted in literature using the term “reddening”. The colour excess represents the effect of extinction on the observed colour index. Its importance arises from the prominence of the intrinsic colour index in determining effective temperature. Higher values of  $(X - Y)$  indicate redder stars, with lower effective temperatures.

The most commonly-used colour index, employed as a reference for most optical observations, is the Johnson  $(B - V)$  index (Johnson & Morgan, 1953). This is due to these filters being the among most widely-used and best-studied available, allowing for better comparisons of different data, including data from older archives.

It can be seen from Equation 1.11 that the luminosity (and therefore flux) of a star is dependent on radius as well as effective temperature. If a plot is made of luminosity against effective temperature (a Hertzsprung-Russell diagram), it can be seen that all stars in a given star cluster follow a single, complex track. Because the stars are approximately the same age in a typical cluster population, this track is known as an isochrone. Isochrones for different population ages and metallicities are calculated using theoretical stellar models, which cover the largest possible spread of initial stellar masses for the required age.

By examining the flux-magnitude equations from both this section and Section 1.1, it becomes clear that both the absolute filter magnitudes and the intrinsic colour indices can be used, together with bolometric corrections, to calculate the luminosity from observational data. To determine the detailed properties of stellar populations, all stars in an observational sample or star cluster are plotted together on a pair of axes known as a colour-magnitude diagram (CMD), which represents an observational analogue of the HR diagram. The absolute magnitude of stars in a given filter  $Z$ ,  $M_Z$ , is on the y-axis, with the flux increasing (and the magnitude value decreasing) upwards. The intrinsic colour index of the stars in two filters  $X$  and  $Y$ ,  $(X - Y)_0$ , is on the x-axis, with the values increasing (and stars becoming redder) to the right. In practice, due to the unknown extinction coefficients of the individual stars and the cluster as a whole, the axial parameters are  $M_{\text{ext},Z}$  and  $(X - Y)$ . Note that filter  $Z$  may be the same as either  $X$  or  $Y$ .

In practice, the universal general shape and position of stellar populations in the HR diagram and each observational CMD, particularly the position and shape of the main sequence, provides a highly useful tool for comparing stellar populations with

unknown distances and extinction coefficients to known examples and to theoretical models. This is done by alignment of the respective main sequences in CMDs, particularly the upper main sequence, which contains the most luminous MS stars and is less sensitive to the (initially unknown) value of the cluster metallicity than the lower MS.

The age of an observed stellar population are determined by, firstly, correcting the data for the effects of distance and extinction and, secondly, aligning a series of isochrones, each of a different age, with the main-sequence (MS) of the observed data. The accepted age of the population is that of the isochrone which most closely follows the progression of stars along the main-sequence turn-off (MSTO). As such, any errors in the estimated extinction can potentially change the age of the best-fit isochrone and therefore produce an erroneous estimate of the true population age.

### Comparing theoretical and observational quantities

For any observational dataset of stars, the stars' individual extinction values will be completely unknown from the data alone. In order to compare observational and theoretical data, the most convenient approach is to add the (theoretical) extinction value(s) to the theoretical dataset magnitudes (i.e., absolute magnitudes), before comparing to the distance-corrected observational data. As a result, the quantity from each dataset that is being compared is the absolute magnitude plus the extinction coefficient in each filter. If we label this quantity  $M_{\text{ext},X}$  for a generic filter  $X$ , we can define it as:

$$M_{\text{ext},X} = M_X + A_X \quad (1.16)$$

Using Equations ?? and ??, Equation 1.16 can now be rewritten such that  $M_{\text{ext},X}$  is defined using both quantities derived directly from observations and those determined by theoretical models:

$$\begin{aligned} M_{\text{ext},X} &= M_X + A_X \text{ (theoretical data)} \\ &= m_X + 5 - 5 \log \left( \frac{d}{\text{pc}} \right) \text{ (observational data)} \end{aligned} \quad (1.17)$$

This allows for direct comparison of theoretical data, whose stars are treated with theoretically-determined  $A_X$  values, with distance-corrected observational data, whose stars have unknown  $A_X$  values. Therefore, this provides a pathway for comparing the standard treatment of extinction (constant  $A_X/A_V$  ratios) with the treatment proposed in this project ( $A_X/A_V$  varying as functions of intrinsic stellar parameters).

### 1.3 The standard treatment of extinction in observed stellar populations

In observations, the extinction for a given source is initially unknown. For a stellar population, observers must make use distinctive features of stellar populations that can be used as standard candles to estimate distance moduli to the population (see Equation ??).

The treatment of extinction in observational surveys is usually via a constant value for the ratio of extinction in a given filter  $X$ , denoted by  $A_X$ , divided by the extinction in the well-studied Johnson- $V$  filter,  $A_V$ . The value used for this ratio, denoted by  $A_X/A_V$ , is often taken from Rieke & Lebofsky (1985). This approach has the significant issue of producing  $A_X/A_V$  values that do not account for variations in the monochromatic flux between stars with different physical parameter values when integrated over the filter's wavelength range, which can be several orders of magnitude. As shown in Figure 1.2, the monochromatic flux at a given wavelength varies greatly with effective temperature, as does the ratio between monochromatic fluxes of stars of different temperatures. This makes the notion that stars of different temperatures lose the same flux in a given filter passband, which is implied by the use constant extinction ratios across all stellar classes, inherently flawed. Stars with higher effective temperatures have emission spectra with much higher and (proportionally greater) fluxes at the shorter wavelengths which are most impacted by interstellar extinction. Therefore, it should be expected that hotter stars experience higher extinctions  $A_X$  for a given filter, not equal values.

Ortolani et al. (2017) used the tabulated extinction ratio tables resulting from Girardi et al. (2008), which demonstrated the significant effect of stellar parameters on the calculated extinction ratios, to search for potential discrepancies in the predicted ages of isochrones after the addition of extinction. This was performed for isochrones with real ages between 12 and 13 Gyr and employed a small selection of Johnson ( $B$ ,  $V$  and  $I$ ) and ACS (F606W, F775W and F814W) broadband filters. They found that, once the assumption of uniform extinction across the entire population was removed by employing the Girardi et al. (2008) data, the isochrone position in the CMD shifted such that, at  $A_V = 1$ , the MSTO of a 12 Gyr isochrone with individual stellar extinction values added is the same as the position of a 12.5 Gyr isochrone with the standard single extinction value added.

### 1.4 Project objective

The first goal of this project is to investigate the variations of the extinction ratios  $A_X/A_V$  in selected photometric filters within multiple filter systems with changes in effective temperature, surface gravity and metallicity. This will be carried out using a

large library of theoretical stellar spectra covering all main stages of stellar evolution. Analytic fitting functions will be employed to model the  $A_X/A_V$  variations as a function of the stellar parameters.

The results of the fitting process will then be applied to the CMD of a representative example of a relatively high-extinction open cluster. The CMD will be fitted with two theoretical isochrones. For the first case, a constant  $A_X/A_V$  value will be applied to the entire isochrone. For the second, varying  $A_X/A_V$  will be applied, using the fitting results. The best estimates for the ages and  $A_V$  values in both cases will be compared, giving a quantitative illustration of the importance of the effect of the stellar parameters on  $A_X/A_V$  ratios used in CMD fitting.

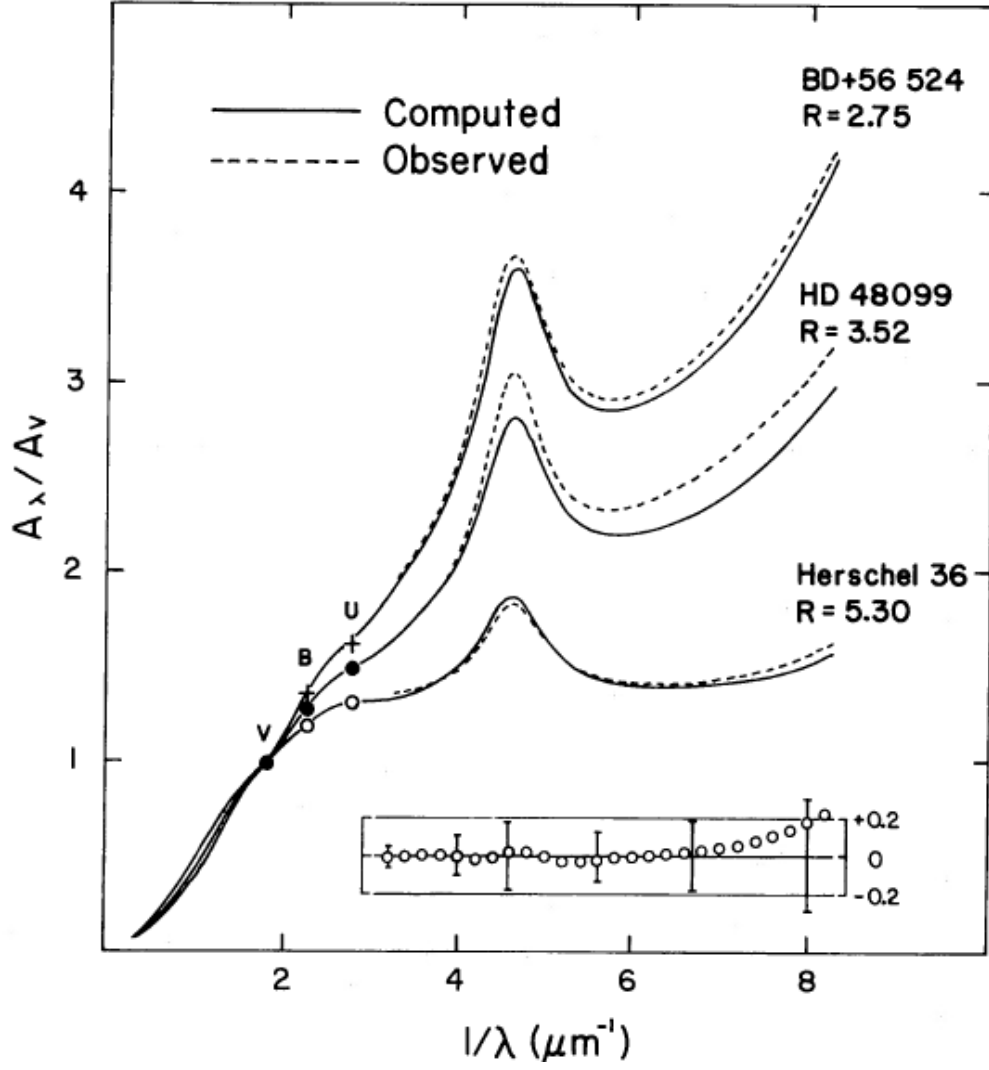


Figure 1.1: Variation of the extinction, normalised to the V-band extinction  $A_V$ , as a function of wavelength, in spectral regions ranging from the IR (left) to the UV (right). The solid lines are calculated using Equation 1.7 at the given  $R_V$  values. These values represent the lines of sight for their respective source stars, which are listed alongside. Source: Cardelli et al. (1989)

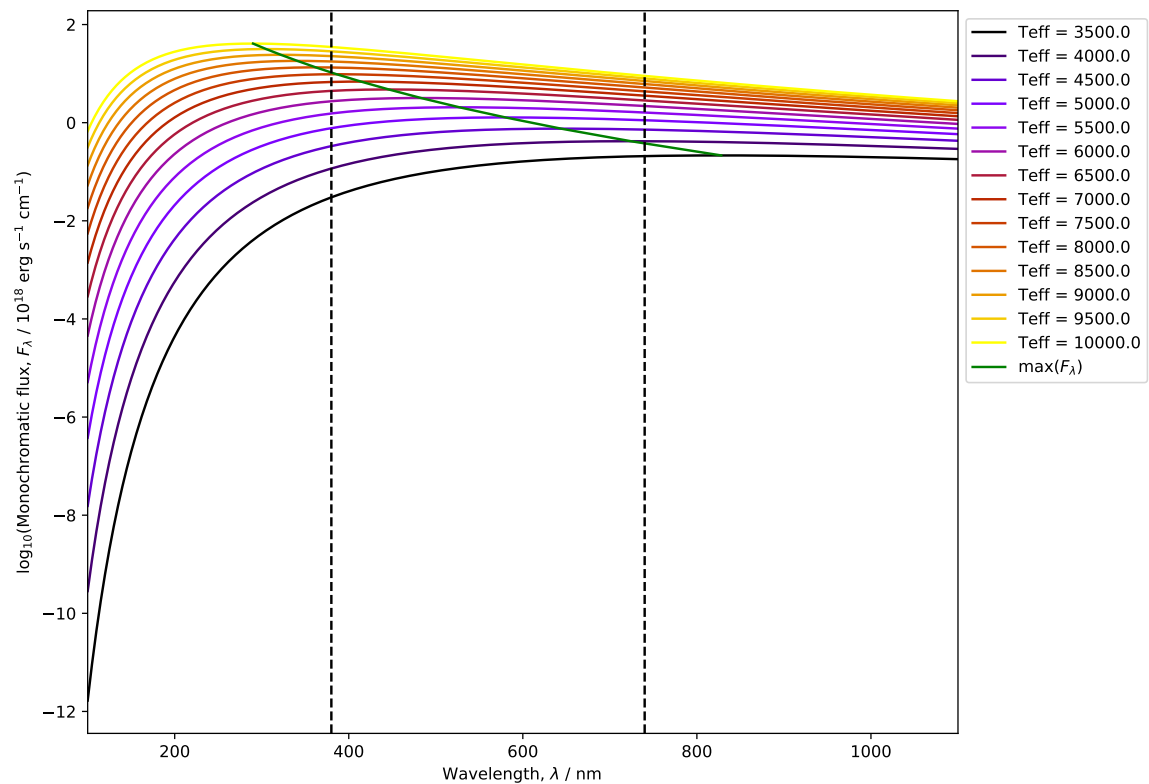


Figure 1.2: Plot of the logarithm of monochromatic flux of a black body for different stellar effective temperatures, as a function of wavelength. The black dashed lines mark the approximate limits of the visible part of the EM spectrum. The green curve represents the variation of the Planck Law maxima with effective temperature.